Supercooled large droplet (SLD) impact on ice at high velocity : splashing characterization

Thomas Alary, Baptiste Dejean, Pierre Berthoumieu, Pierre Trontin

Supercooled large droplet (SLD) impact on ice at high velocity : splashing characterization

T. Alary [(a)]*, B. Déjean [(a)], P. Berthoumieu [(a)], P. Trontin [(b)]
[(a)] *ONERA/DMPE–Université de Toulouse, F-31055 Toulouse, France*
[(b)] *Univ Lyon, Univ Claude Bernard Lyon 1, CNRS, Ecole Centrale de Lyon, INSA Lyon, LMFA, UMR5509, 69622 Villeurbanne, France*

The present paper deals with the impact of supercooled large droplets (SLD) at high velocity on walls of different characteristics (smooth/clean substrate vs. rough/iced surface resulting from continuous ice accretion). A visualization technique of the impact is presented to track and observe the splashing event over time. A focus is proposed on the characterization of the re-emitted droplets after the impact, especially on the particle size, velocity and ejection angle distributions. The experiments are conducted in the ONERA icing wind tunnel which allows to reach regimes where the Weber number is of the order of 160 000, which extends the range of velocities usually found in the literature to characterize the impact of SLD.

I. Introduction

The impact of liquid droplets on solid surfaces is a common phenomenon in nature, and its physical understanding is fundamental for a wide variety of technical applications. One of them is aircraft icing. Icing occurs when an aircraft flies through a cloud in which supercooled droplets are suspended with an ambient air temperature below the freezing point. Wings, motors intakes or probes can hit droplet in suspensions. The droplets impinge on the aircraft surfaces and freeze, leading to ice accretion. When impacting a wall at high velocity, a drop may splash leading to the ejection of many small droplets. The characterization of the secondary droplets re-emitted in the gas flow is of great interest for the configurations where these particles can impact again a downstream surface (case of cascade geometrical settings or wings with high-lift elements for instance).

Drop impact on walls has already been the subject of numerous studies in the past [1–4]. The physics of drop impact requires more investigation to complete this knowledge, especially for very high speed impact velocity. A deep understanding and an accurate modelling of drop impact is a prerequisite for simulating icing phenomena related to the supercooled large droplets. Impact on dry surfaces can be subdivided into fives distinct regimes [5] (figure 1):

- Deposition : the drop spreads out and stays attached to the surface during all the entire phenomena without breakup.
- Corona splash : the liquid spreads on the surface and separates forming a crown lamella. This lamella breaks up into secondary droplets.
- Prompt splash : droplet generation at the early beginning of the spreading phase. Droplets are ejected from finger jets formed directly at the surface without corona formation.
- Rebound and partial rebound : these regimes are observed only when a receding phase occurs with high inertia droplets.

The objective of this paper is twofold. First, the impact of SLD is studied for lower temperatures and higher impact velocities compared to previous experiments [2]. The range for the Weber (We) number values is thus extended from 20 000 (previous works of [2]) to 160 000. A wide range of air temperature is also investigated from -20°C to 5°C whereas in the past studies experiments where realized at ambient air temperature [2, 6, 7]. The second objective is to study the influence of the wall properties on the droplet impact. More precisely, the impact on a smooth and dry surface will be compared with the one on a wall covered by ice. Previous studies concerning SLD and surface properties focused on impact on blotter paper and determination of the mass deposition rate but did not focused on the diameter and velocities of the re-emitted droplets [8, 9]. This information is complementary to the deposition rate in the computation of ice shapes in order to determine the trajectories of the re-emitted droplets and the surfaces likely to be reached by secondary droplets resulting from a first impact upstream.

*Corresponding author: thomas.alary@onera.fr

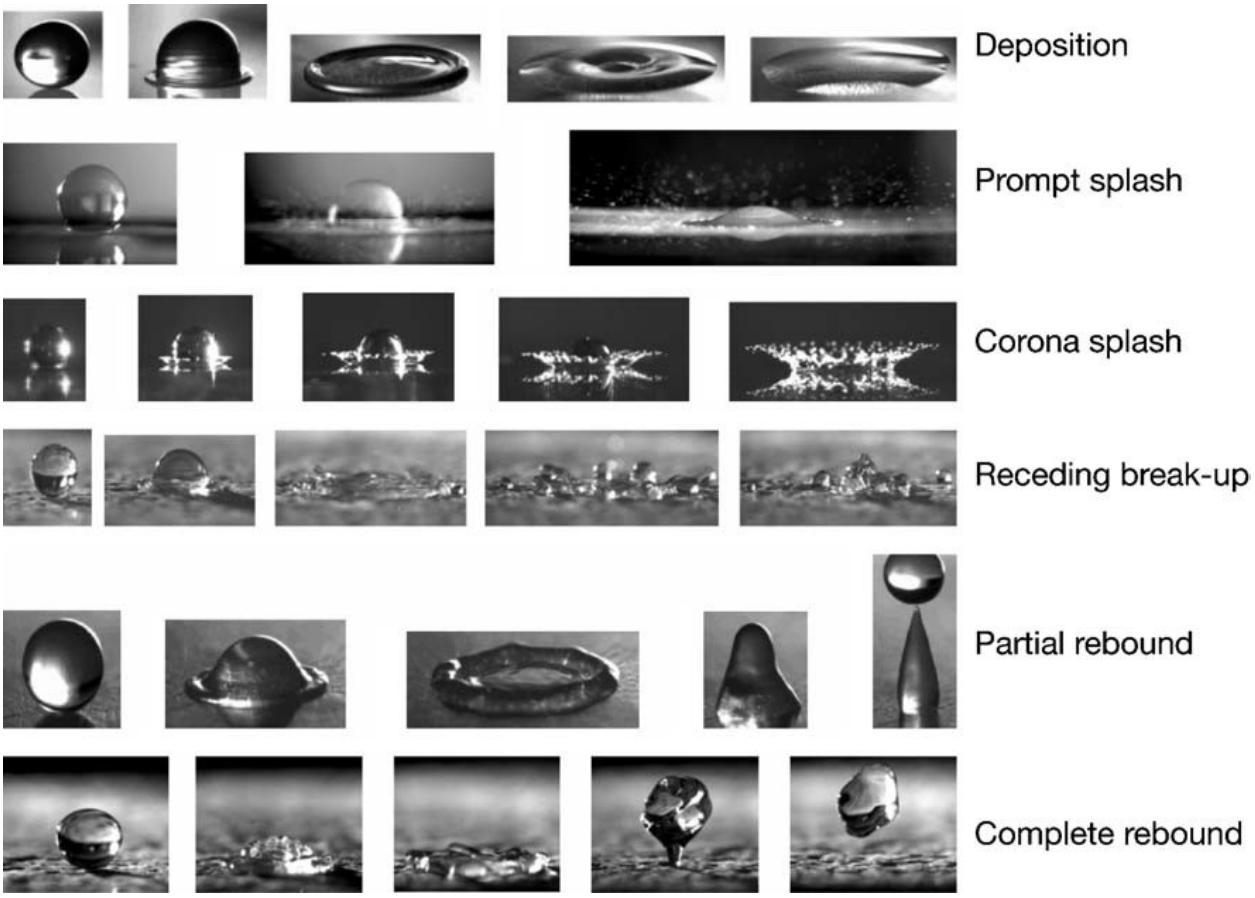

Fig. 1 Illustration of different impact regimes. Reprinted from [5].

II. Experimental set-up

A. Icing wind tunnel and drop generation

Experiments are conducted in the ONERA icing wind tunnel (Fig. 2). This is a vertical closed loop wind tunnel

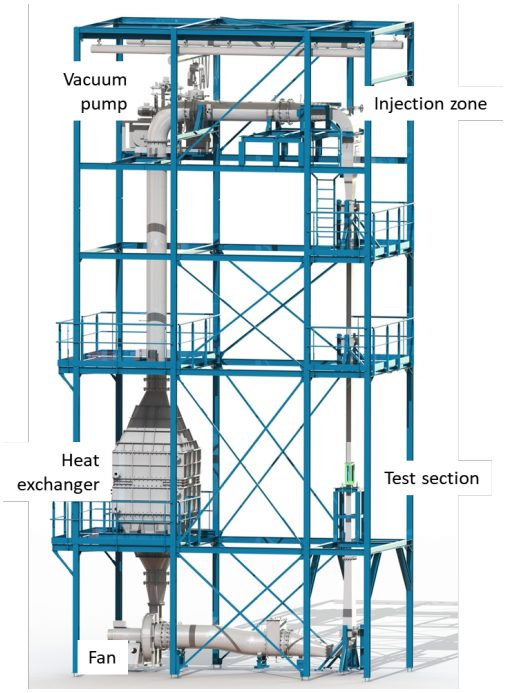

Fig. 2 ONERA Icing Wind Tunnel. The test section is a 10 cm x 20 cm x 50 cm rectangular cuboid. The four sides can receive transparent windows allowing visualizations or optical measurements.

dedicated to SLD studies. It was designed to have droplets with a maximum diameter of 330 µm at the equilibrium with the airflow at a maximum of 150 m/s. Although the velocity profile across the rectangular test section (100 x 200 mm^2) is not highly uniform due to the use of a long convergent nozzle for droplet acceleration up to 190 m/s and the development of boundary layers along the walls, the mockup is however placed near the center of the vein where the air velocity is measured to be constant close to $x = y = 0$ (Figs. 3a and 3b). The characterization of the velocity profiles has been done with a Kiel probe positioned along the center of each side of the test vein.

Droplets are generated inside the wind tunnel by a TSI MDG100 drop generator by applying a mechanical excitation on a thin liquid jet of water. The excitation is provided by a piezoelectric ceramic driven by a function generator. The droplet size is directly linked to the excitation frequency imposed at the ceramic, the diameter of the liquid jet itself fixed by the exit pinhole of the injector, and the liquid flow rate. After being generated, the droplets enter the airflow which is accelerated in a convergent pipe between the injection zone and the test section. A characterization of the droplets cloud has been done and the maximum droplet density is observed at a position shifted 1 cm in the x direction.

In Fig. 4a, the model consists of a 10 mm aluminium pipe with a 3 mm flat edge placed horizontally in the wind tunnel (Fig. 4b). Droplets impact on the flat edge whose characteristic dimensions are much larger than those of the largest droplets generated. Thus, locally on that flat surface, the impact of the droplets can be considered as an impact on a flat plate. For aerodynamic reasons, a pipe is used at the back of the model.

B. Drop impact visualization

In addition to classical wind tunnel instrumentation (pressure and temperature probes), optical diagnostic has been used to observe the phenomenon of high speed drop impact (Fig. 7). The impact is captured using a PIV (Particle Image Velocimetry) camera. Droplet impact visualizations have been done by shadowgraphy with a camera and a laser diode with very short flashes duration placed on either side of the object to be observed. With these conditions, droplets appear dark on a light background. The key difficulty of visually tracking the impact comes from the synchronization

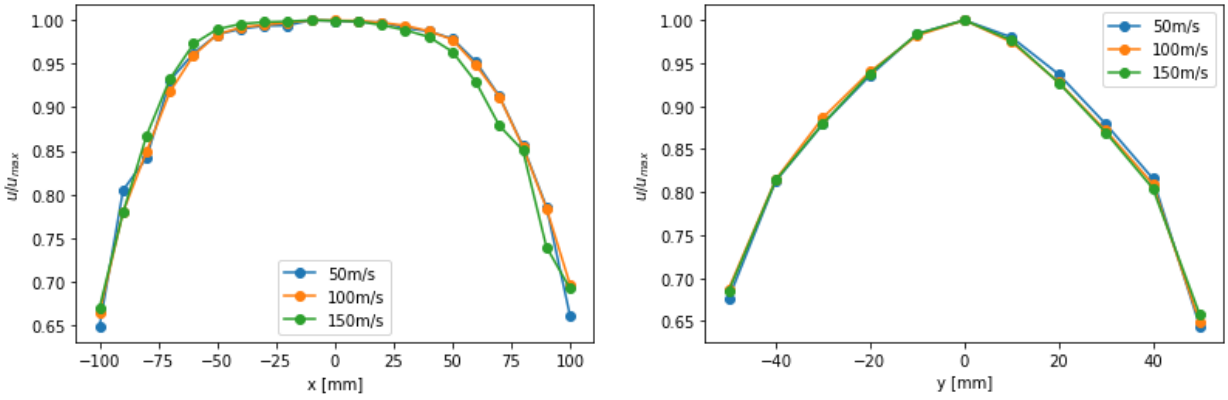

(a) Velocity profile of the test section for 50 m/s, 100 m/s and 150 m/s for $y = 0$.

(b) Velocity profiles along the transverse direction section for 50 m/s, 100 m/s and 150 m/s for $x = 0$.

Fig. 3 Velocity profiles measured in th ONERA icing research wind tunnel

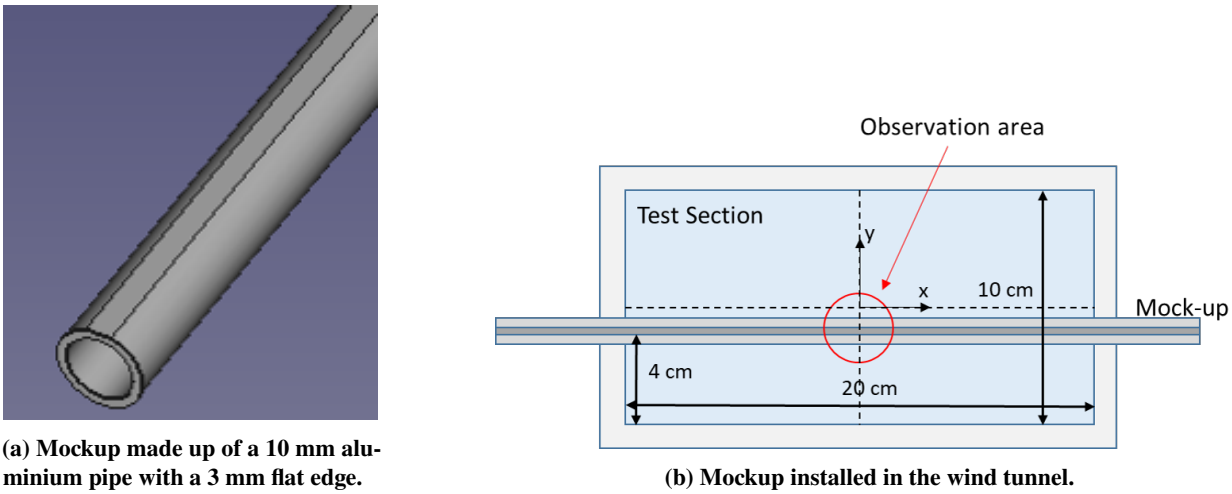

(a) Mockup made up of a 10 mm aluminium pipe with a 3 mm flat edge.

(b) Mockup installed in the wind tunnel.

Fig. 4 Geometrical characteristics of the model and installation in the icing wind tunnel.

between the image capture and the presence of a drop in the field of view. Since the droplet density in the gas flow is low with a volume fraction of the order of 10^{-6}, the probability of a droplet crossing the field of view of the camera is low. To overcome this difficulty, a system for detecting the presence of the droplets in the field of the camera is used, just before it enters the field of view of the camera characterized by a surface of a few millimeters long and a few tenths of a millimeter deep (Fig. 5). The detection system consists of a laser beam ("Laser" in Fig. 5) which illuminates an area

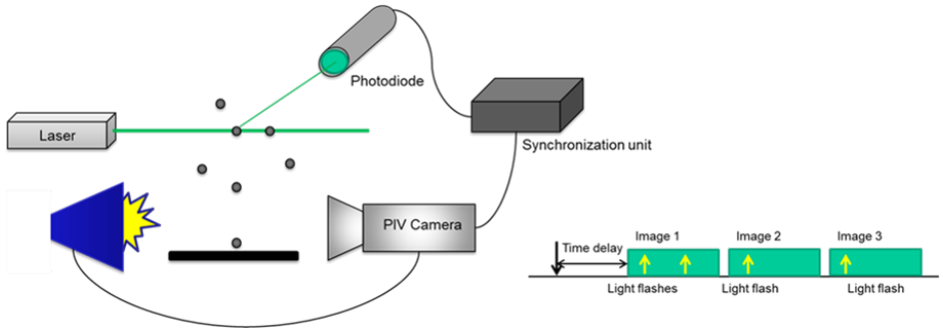

Fig. 5 Droplet detection and visualization system

upstream of the impact zone, depicted by the green beam in Fig. 5. When the impinging droplets cross this area, the light scattered by the droplets running through the beam is collected by a photosensitive element (denoted "Photodiode" in Fig. 5) positioned in mode *front scattering* to collect the maximum amount of light. The generated electrical signal from the detection photodiode is then sent to the lighting system (in blue in Fig. 5) and the PIV camera, to illuminate and visualize the impact of the droplet on the wall. To enable time synchronization, a latency is added to take into account the travel time of the droplet from the detection system to the wall.

Regarding the visualization system, a PIV camera JAI BM131GE with a resolution of 1296 x 966 square pixels of 3.75 µm sides is used for the image acquisition. It is associated with a Cavilux lighting system (laser diode). This camera offers a good resolution compared to very high speed cameras but it allows to record only three successive images (Fig. 7) at a high frequency, with an interval between two successive images that can go down to 1.5 µs. As the entire dynamics of the impact cannot be recorded at one time, the sequence of three successive images is used to describe the impact of the droplets. The first image is used to describe the characteristics of the incident droplet. To do this, two light flashes illuminate the droplet successively and the droplet appears twice on the same image. From the time delay between the two flashes, the velocity of the incident droplet can be determined by image processing. The last two images are taken at two different later times whose interval is adjusted by the incident velocity of the droplets. These images are used to both observe and characterize the droplet impacts.

C. Secondary droplet characterization

The characterization of the secondary droplets re-emitted after impact on the mock-up is performed by a Phase Doppler Analyser (PDA). This optical non-intrusive system measures the diameter and the two components of the velocity of the spherical particles passing through its measurement volume. The measurement volume is the result of the intersection between two laser beams. The system used is a Dual PDA from Dantec. The probe volume has been positioned 1 mm above the impingement surface and this position has been adjusted for each mock-up and each airflow velocity since the airflow exerts an aerodynamic load on the mock-up which tends to displace vertically the impingement surface. This distance is the result of a compromise between the need for the PDA to be close enough to the wall to have access to a sufficient number of re-emitted droplets, and the need to move back from the wall to avoid that the PDA interacts with macro structures that can appear at the wall as during a corona splash. The sample size is limited to 20 000 acquired droplets, in order to have representative values of the phenomenon observed.

During the measurement campaigns, all the droplets crossing the probe volume have been taken into account whatever their trajectory. However, two populations of droplets are counted by the PDA system if no particular care is taken. The first one is represented by secondary droplets ejected outward the wall. The second one represents also re-emitted droplets but, due to the carrier flow, they are pulled back in and oriented towards the impingement surface. Only the droplets leaving the wall are then selected (first population of droplets). The criterion used is the orientation of the velocity vector with respect to the normal vector to the wall.

III. Results

A. Observation and qualitative analysis of the impact

Many studies have proposed splashing parameter to determine a splashing threshold. Riboux and Gordillo [7] relate splashing to an aerodynamic lift force acting on the spreading lamella. When this lift force is higher than the capillary retraction, splashing is expected. They proposed a parameter $\beta = \sqrt{F_L/(2\sigma)}$ to characterize the threshold between splashing and no splashing, where F_L is the lift force and σ the surface tension coefficient. From experiments in [3], the criterion $\beta > 0.19$ is proposed when splashing is expected. In this study, β is ranged between 0.2 and 1.2 (Fig 6) so that splashing is expected according to the β criterion [10], whatever the nature of the impact surface since the parameter β does not consider the properties of the substrate (clean or iced substrate).

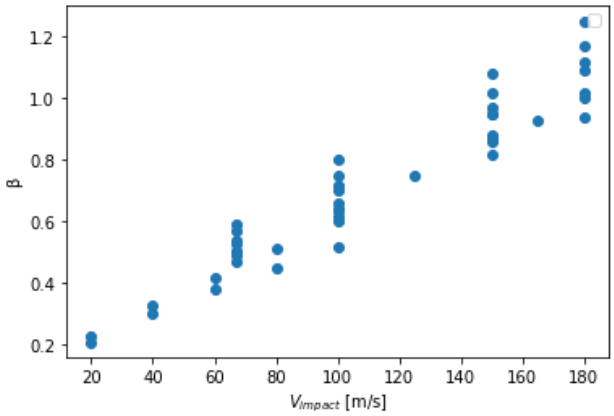

Fig. 6 Value of β in function of the drop impact velocity for experiments investigated in this paper. Different airflow velocities are shown.

In the present study, prompt splash is observed on smooth surfaces (Fig. 7a), whereas corona splash is observed for impacts on glaze or rime ice shapes (Figs. 7b and 7c), with a rougher substrate. Corona and prompt splashes have a different morphology. In case of corona splash, secondary droplets are produced by finger jets themselves issued from a liquid sheet (Figs. 7b and 7c). Regarding prompt splash (Fig. 7a), the secondary droplets are ejected directly from the surface without the formation of a liquid rim or sheet.

If one focuses on the direction of the re-emitted liquid structures, it is rather vertical for the finger jets in the case of a corona splashing (Figs. 7b and 7c), whereas the re-emitted droplets for prompt splash (Fig. 7a) are ejected with a larger and grazing ejection angle.

B. Secondary droplet characterization

The influence of the nature of the substrate (clean/smooth vs. iced/rough) is studied on the characteristics of the re-emitted secondary droplets. The experimental set-up needs to be adapted for the impact on an iced substrate under icing conditions. Indeed, as the ice layer thickness increases with time due to ice accretion, the position of the PDA probe needs to be updated at any time in order to secure a constant distance of 1 mm between the PDA probe and the continuously updated impingement surface. This is achieved through the use of a video camera which records ice accretion in real time.

In this paper, only normal impacts are considered. Figure 8 shows the arithmetic mean diameter d_{10} of the secondary re-emitted droplets scaled by the arithmetic mean diameter D_0 of the incidents droplets as a function of the normal Weber number We_n.

The average diameter d_{10} depends on the nature of the substrate on which the droplets impact with a larger value for d_{10} after an impact on a rough iced surface compared to the impact on a smooth clean surface. Whatever the nature of the substrate, d_{10} is a decreasing function of We_n. This is in agreement with the measurements made in [2, 7, 11] (Fig. 9). The present study also extend for higher Weber number this result. For a given substrate type, Fig. 8 shows that the temperature has no influence on the characteristics of the re-emitted droplets. Here, thermal equilibrium is assumed between the air and the droplets.

(a) Impact on a dry and smooth surface at 150 m/s.

(b) Impact on a glaze ice surface at 150 m/s in an airflow cooled at -2°C.

(c) Impact on a rime ice surface at 150 m/s in an airflow cooled at -5°C.

Fig. 7 Impact of droplets with diameters of approximately 330 µm. Influence of the nature of the substrate.

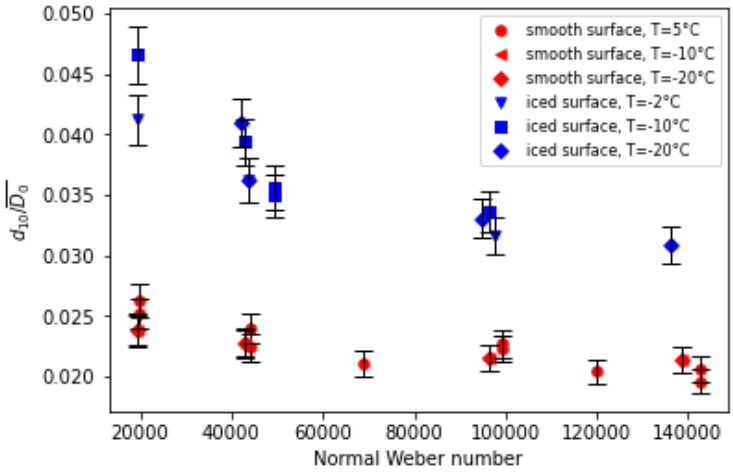

Fig. 8 Arithmetic mean diameter d_{10} of the secondary droplets scaled by the arithmetic mean diameter D_0 of the incidents droplets in function of the normal Weber number We_n.

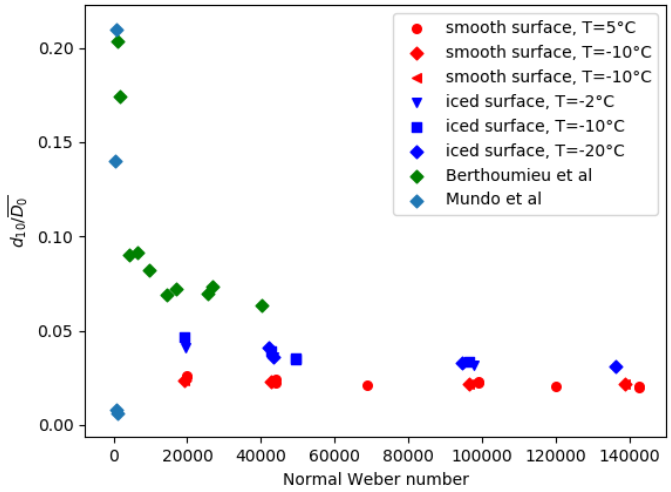

Fig. 9 Experimental data for the arithmetic mean diameter d_{10} of the secondary droplets scaled by the arithmetic mean diameter D_0 compared to previous experiments

In addition to the mean diameter d_{10} (Fig. 8), the particle size distributions (PSD) of the re-emitted droplets are shown in Fig. 10. PSD are obtained with the PDA with which 20 000 drops are visualized. Among the droplets retained

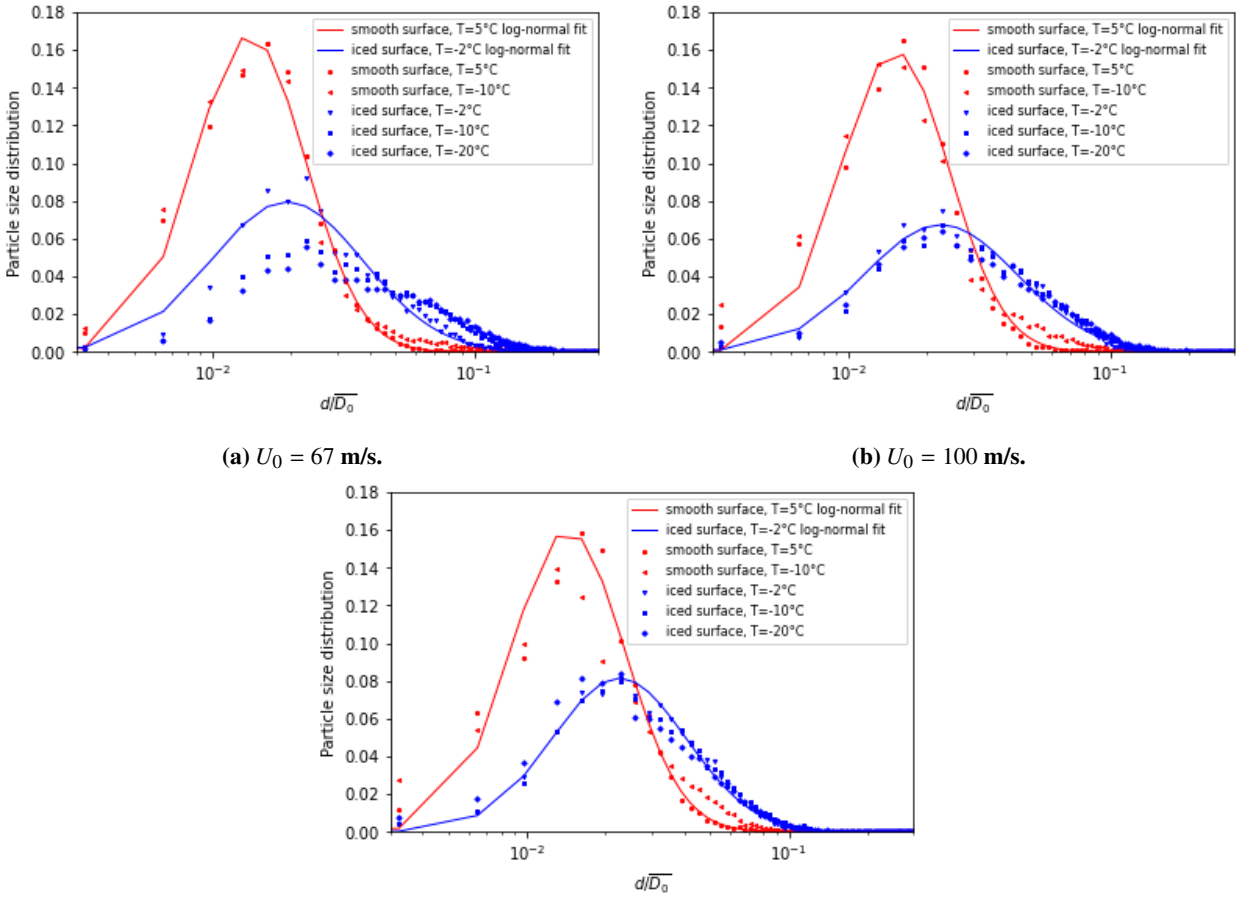

(a) $U_0 = 67$ **m/s.**

(b) $U_0 = 100$ **m/s.**

(c) $U_0 = 150$ **m/s.**

Fig. 10 Particle size distributions (PSD) of the re-emitted droplets after a normal impact. $D_0 = 330$ **µm. Symbols: experiments. Solid lines: fitting with log-normal laws. The influence of the nature of the substrate is studied (red for a clean/smooth surface and blue for a rough/iced surface). Additionally, for each type of substrate, the influence of its temperature is studied. Different impact velocities** U_0 **are proposed.**

to build the statistics (about half of the drops visualized by the PDA), some of them leaving the wall cross the probe volume with an ascendant trajectory. The others, moving towards the wall, cross the probe volume with an descendant trajectory. The latter are rejected to derive the statistics for the re-emitted droplets. The PSD confirm the results in Fig. 8, namely that the re-emitted droplets are smaller after an impact on smooth/clean substrate than an impact on a rough/iced substrate. These conclusions are to be compared with those of [12] where the dependency between the diameter of the re-emitted droplets and the nature of the splashing is discussed. In this study, the re-emitted droplets are shown to be smaller for impacts with prompt splashing whereas they are larger for impacts with corona splashing. This is consistent with the observations of Sec. III.A and Fig. 7 where prompt slashing is observed when impacting an smooth/clean wall (leading thus to smaller re-emitted droplets), while corona splashing is observed for impacting a rough/iced wall (leading to larger re-emitted droplets). Another observation in Fig. 10 is about the level of dispersion of the re-emitted droplet diameters. For impacts on a rough/iced wall, the PSD of the re-emitted droplets are more dispersed than for impacts on a smooth/clean wall.

Regarding the distribution of the norm of the velocity after impact, Fig. 11 shows the particle velocity distributions of the re-emitted droplets after a normal impact. The influence of the nature of the substrate is studied for different impact velocities U_0. First of all, it can be noted that the velocities of some ejected droplets exceed the incoming

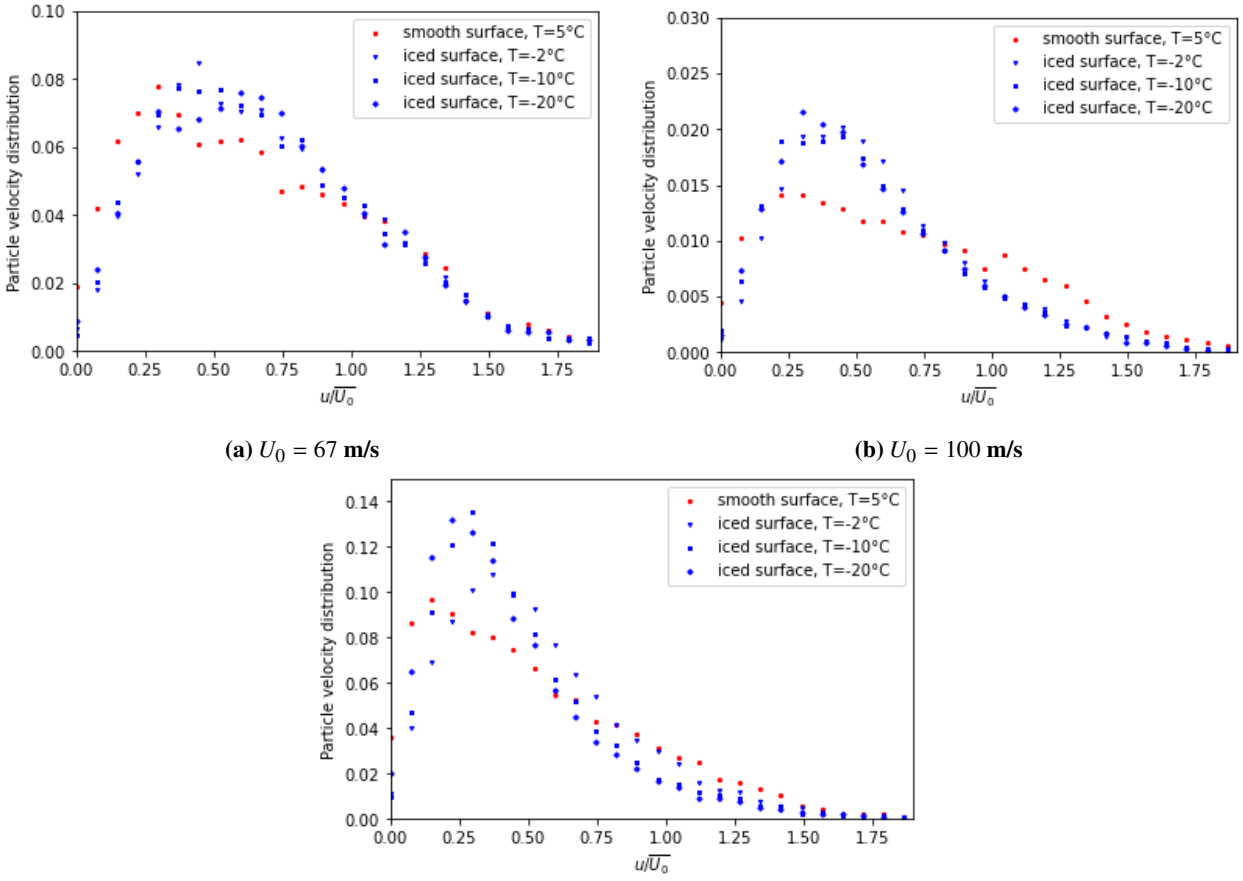

(a) $U_0 = 67$ **m/s**

(b) $U_0 = 100$ **m/s**

(c) $U_0 = 150$ **m/s**

Fig. 11 Particle velocity distributions of the re-emitted droplets after a normal impact. $D_0 = 330$ **µm. The influence of the nature of the substrate is studied (red for a clean/smooth surface and blue for a rough/iced surface). Additionally, for each type of substrate, the influence of its temperature is studied. Different impact velocities** U_0 **are proposed.**

droplet velocity U_0, which has already been observed in [4, 12]. For an impact on a smooth/clean surface, the velocity dispersion of the re-emitted droplets is greater than for an impact on a rough/iced surface. For the highest impinging velocities (U_0 = 100 m/s and U_0 = 150 m/s), the typical velocity of the re-emitted droplets is of the order of $u/U_0 \approx 0.25$ for rough/iced substrates. Note that the temperature has no influence.

In addition to the velocity norm, the particle ejection angle is studied to characterize the velocity vector of the re-emitted droplets. Figure 12 shows the particle ejection angle distribution of the re-emitted droplets after a normal impact for different substrates. For clarity, Fig. 13 summarizes the definitions of the impact i and ejection r angles. The

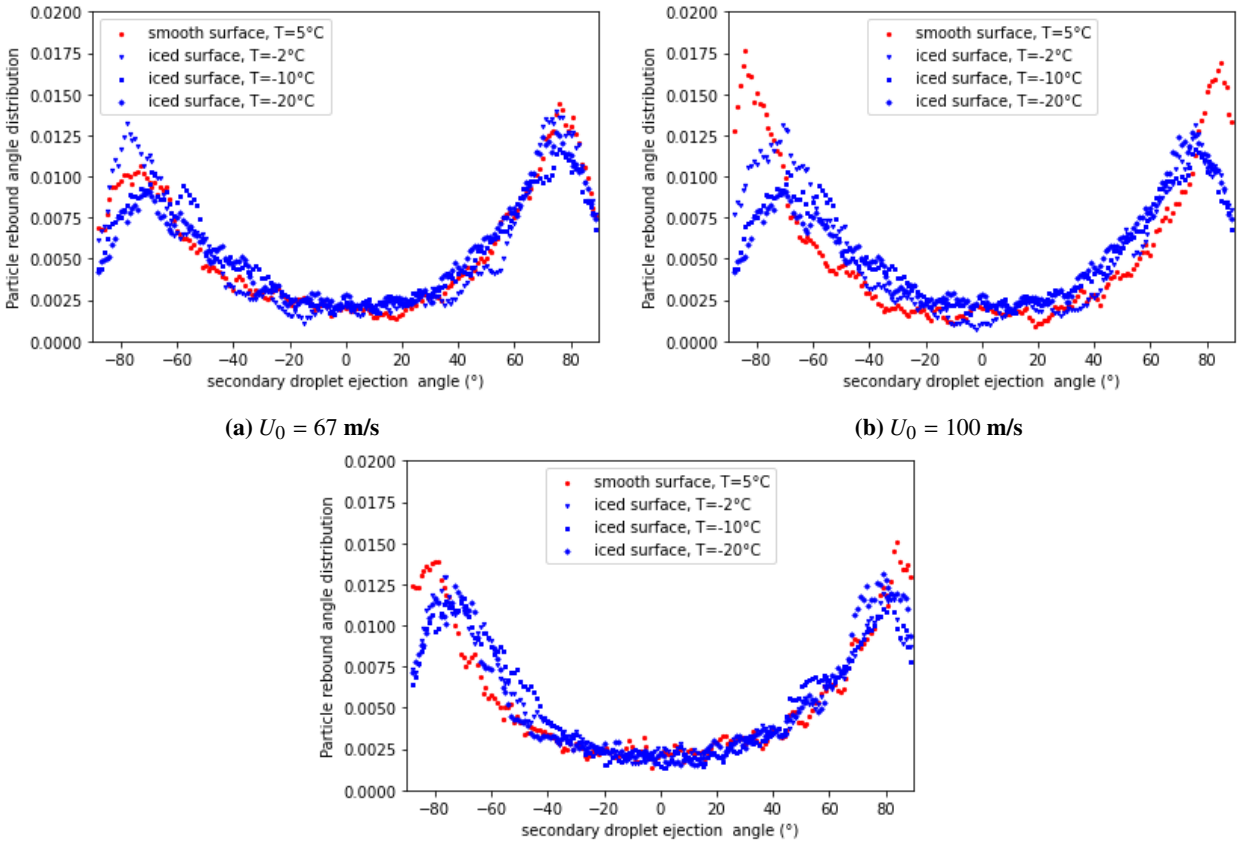

(a) U_0 = 67 **m/s**

(b) U_0 = 100 **m/s**

(c) U_0 = 150 **m/s**

Fig. 12 Particle ejection angle distributions of the re-emitted droplets after a normal impact. D_0 = 330 **µm. The influence of the nature of the substrate is studied (red for a clean/smooth surface and blue for a rough/iced surface). Additionally, for each type of substrate, the influence of its temperature is studied. Different impact velocities** U_0 **are proposed.**

ejection angle r is determined from the measurement of the two components of the droplet velocity. The influence of the nature of the substrate is studied for different impact velocities U_0. For the two highest impact velocities U_0 = 100 m/s and U_0 = 150 m/s, the number of re-emitted grazing droplets (corresponding to $|r| \geq 80°$) is larger for impacts on smooth/clean substrates with prompt splashing than for impacts on rough/iced substrates with corona splashing. Thus, regarding these grazing re-emitted droplets after impact on a smooth/clean substrate, they spend more time near the wall, in a zone where the viscous effects are important because of the presence of a boundary layer. This may explain the higher deceleration of the secondary droplets in the case of an impact on a smooth/clean surface. This hypothesis, proposed in [4], will be confirmed hereinafter.

Figure 14 shows three different features for droplets re-emitted after a normal impact on a wall. Each symbol represents the diameter d/D_0 and the velicity u/U_0 for a given re-emitted droplet in the cloud. In addition, each symbol is colored by the value of the ejection angle r. For an impact on a smooth surface where prompt splash is promoted, there is a correlation between the velocity magnitudes of the re-emitted droplets and their ejection angles. The fastest

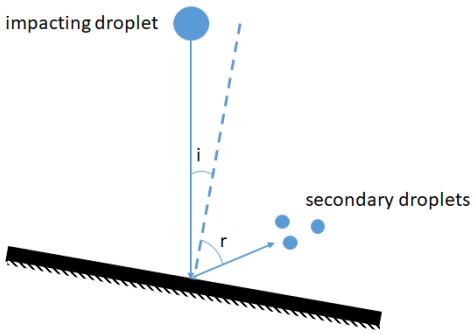

Fig. 13 Definition of the impact i and ejection r angles.

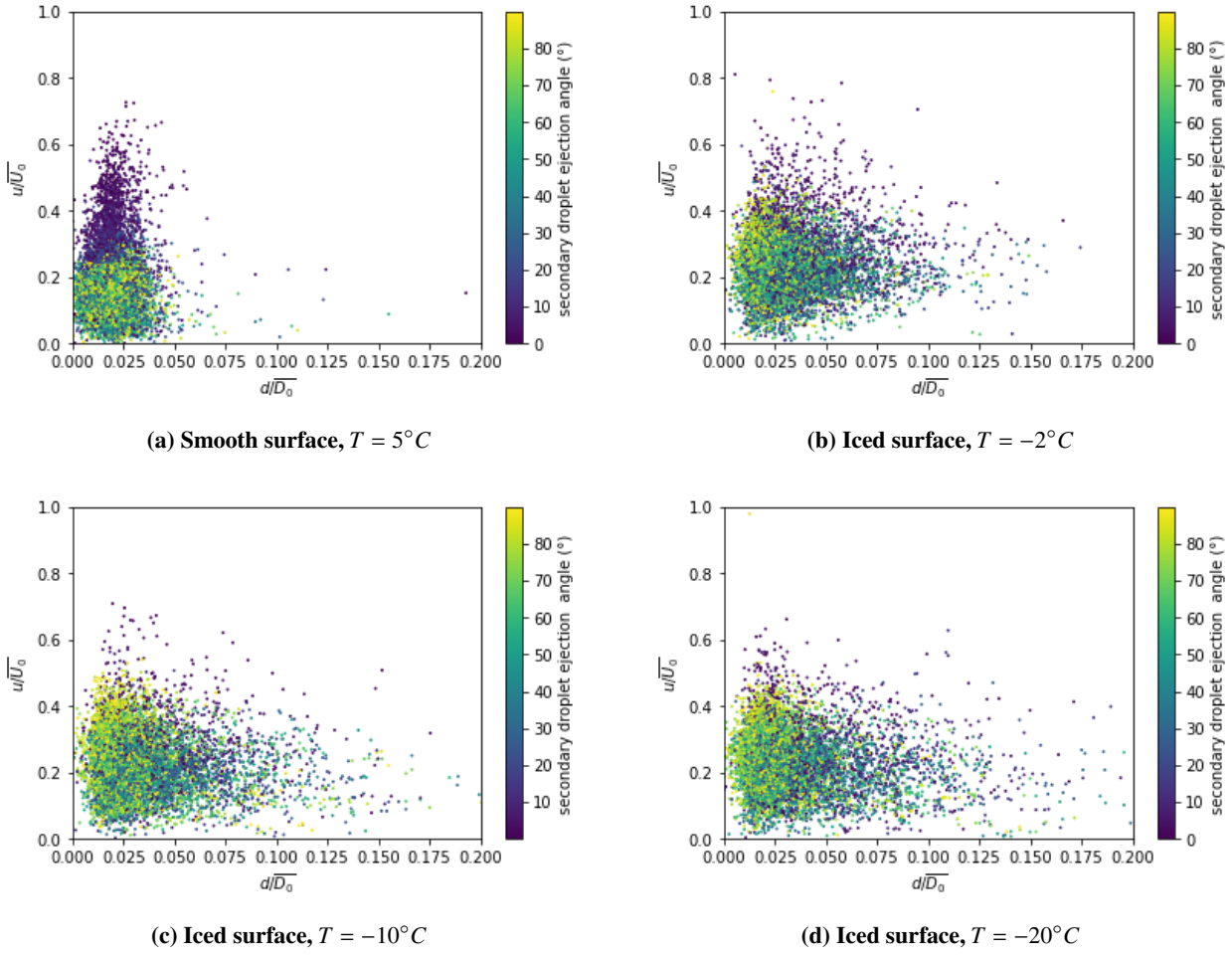

(a) Smooth surface, $T = 5°C$

(b) Iced surface, $T = -2°C$

(c) Iced surface, $T = -10°C$

(d) Iced surface, $T = -20°C$

Fig. 14 u/U_0 vs. d/D_0 for each re-emitted droplet. Each symbol, additionally colored by the ejection angle r, represents a re-emitted droplet in the cloud. $D_0 = 330$ µm. $U_0 = 100$ m/s.

droplets are those with the smallest ejection angle, i.e. those re-emitted perpendicular to the wall. This is in agreement with the experiments made in [3, 7] and with the previous hypothesis that a grazing re-emitted droplet spends more time close to the wall in the boundary layer region and thus experiences a larger deceleration.

Regarding the impact on an rough/iced surface, the particle size distributions of the re-emitted droplets is wider, which is in line with Fig. 10. The bouncing angle r is correlated with the re-emitted particle diameter. For low values of r (direction of re-emission almost normal to the wall), the re-emitted droplets are larger. This is in agreement with our visualizations (Figs. 7b and 7c) where the largest re-emitted droplets are generated by the finger jets and ejected rather vertically.

IV. Conclusion

The experimental techniques presented in this paper met the challenge of measuring quantities at small scales (re-emitted droplet diameters, velocities and bouncing angles) with a high accuracy, for high impact velocities and in a confined environment (icing wind tunnel). Cameras and PDA were used to visualize and analyse the outcome of the splashing event. The visualizations showed the influence of the nature of the substrate on the type of splashing observed. For impacts on a smooth/clean surface, prompt splashing is observed, whereas corona splashing is observed for impacts on a rough/iced surface. It was also observed that the nature of the substrate has an influence on the size, velocity and ejection angle distributions of the re-emitted droplets. The experiments conducted in this study extended to higher impact velocities the tendencies observed in the existing literature at lower Re-number. This is for instance the case for the decrease of the mean diameter of the re-emitted droplets as a function of the Weber number.

Acknowledgments

This project has received funding from the European Union's Horizon 2020 research and innovation programme under grant agreement No 824310.

References

[1] Berthoumieu, P., "Experimental study of supercooled large droplets impact in an icing wind tunnel," *4th AIAA Atmospheric and Space Environments Conference*, 2012, p. 3130.

[2] Berthoumieu, P., and Déjean, B., "Experimental investigation of SLD impact phenomena," *7th European conference for aeronautics and space sciences (EUCASS)*, 2017.

[3] Burzynski, D. A., Roisman, I. V., and Bansmer, S. E., "On the splashing of high-speed drops impacting a dry surface," *Journal of Fluid Mechanics*, Vol. 892, 2020. ISBN: 0022-1120 Publisher: Cambridge University Press.

[4] Thoroddsen, S. T., Takehara, K., and Etoh, T. G., "Micro-splashing by drop impacts," *Journal of Fluid Mechanics*, Vol. 706, 2012, pp. 560–570. https://doi.org/10.1017/jfm.2012.281, URL https://www.cambridge.org/core/product/identifier/S0022112012002819/type/journal_article.

[5] Rioboo, R., Tropea, C., and Marengo, M., "OUTCOMES FROM A DROP IMPACT ON SOLID SURFACES," *Atomization and Sprays*, Vol. 11, No. 2, 2001, p. 12. https://doi.org/10.1615/AtomizSpr.v11.i2.40, URL http://www.dl.begellhouse.com/journals/6a7c7e10642258cc,02b3b3196bd0e2a7,4224940d1f16de7f.html.

[6] Burzynski, D. A., and Bansmer, S. E., "High speed visualization of droplets impacting with a dry surface at high weber numbers," *New Results in Numerical and Experimental Fluid Mechanics XI*, Springer, 2018, pp. 511–521.

[7] Riboux, G., and Gordillo, J. M., "The diameters and velocities of the droplets ejected after splashing," *Journal of Fluid Mechanics*, Vol. 772, 2015, pp. 630–648. ISBN: 0022-1120 Publisher: Cambridge University Press.

[8] Bodoc, V., Berthoumieu, P., and Déjean, B., "Experimental Investigation of Large Droplet Impact with Application to SLD Icing," *Microgravity Science and Technology*, Vol. 33, No. 5, 2021, p. 59. https://doi.org/10.1007/s12217-021-09900-9, URL https://link.springer.com/10.1007/s12217-021-09900-9.

[9] Papadakis, M., Rachman, A., Wong, S.-C., Bidwell, C., and Bencic, T., "An Experimental Investigation of SLD Impingement on Airfoils and Simulated Ice Shapes," 2003, pp. 2003–01–2129. https://doi.org/10.4271/2003-01-2129, URL https://www.sae.org/content/2003-01-2129/.

[10] Riboux, G., and Gordillo, J. M., "Experiments of drops impacting a smooth solid surface: a model of the critical impact speed for drop splashing," *Physical review letters*, Vol. 113, No. 2, 2014, p. 024507. Publisher: APS.

[11] Mundo, C. H. R., Sommerfeld, M., and Tropea, C., "Droplet-wall collisions: experimental studies of the deformation and breakup process," *International journal of multiphase flow*, Vol. 21, No. 2, 1995, pp. 151–173. ISBN: 0301-9322 Publisher: Elsevier.

[12] Burzynski, D., "On the Impact of High-Speed Drops on Dry and Wetted Surfaces," Ph.D. thesis, 2021.